Thermochimica Acta 367–368 (2001) 101–106

thermochimica acta

www.elsevier.com/locate/tca

DSC and DEA studies of underfill curing kinetics

Yi He*

Assembly Test Materials Operation, Assembly Materials Characterization Laboratories, CH5-232,
Intel Corporation, 5000 W. Chandler Blvd., Chandler, AZ 85226-3699, USA

Received 13 October 1999; accepted 11 May 2000

Abstract

Isothermal and non-isothermal differential scanning calorimetry (DSC) and dielectric analysis (DEA) techniques were used to study the curing kinetics of an epoxy-based underfill material used in electronic packaging. Based on the phenomenological kinetic analyses, the activation energy for the curing reaction determined from the non-isothermal DSC studies is similar to that obtained from the isothermal DSC experiments. DEA and rheological analyses demonstrated that the DEA loss factor peak can be used to monitor the gelation. In addition, our results reveal that the activation energy determined by DEA experiments (both isothermal and non-isothermal) correlates well with the DSC results. © 2001 Elsevier Science B.V. All rights reserved.

Keywords: DSC; DEA; Kinetics

1. Introduction

Underfill encapsulants are commonly used in advanced microelectronic packaging to reduce the thermal expansion mismatch between the silicon chip and the organic substrate, thus improving solder-joint reliability [1,2]. Underfill encapsulants have many advantages, such as to redistribute the stresses and strains over the entire silicon chip area, and to protect the chip from moisture, contamination, and other hostile environments. However, one serious disadvantage of underfill encapsulant is the reduction of manufacturing throughput. In fact, the underfilling process becomes the bottleneck in the flip-chip attachment process [3,4]. Therefore, fast-flow, fast-cure underfill encapsulants are actively developed to improve manufacturing throughput and to support high volume manufacturing. Consequently, understanding the curing behavior of underfill encapsulant is critical to optimizing the manufacturing process. The kinetics information can also be used to predict material pot life at processing temperatures.

Previously, we reported the physical properties of an epoxy-based underfill encapsulant used in Intel's advanced packaging [5]. In this study, differential scanning calorimetry (DSC) and dielectric analysis (DEA) techniques were applied to investigate the curing kinetics of an epoxy-based underfill encapsulant used for Intel's advanced flip-chip packages. The study of underfill curing kinetics is of practical importance, because knowing the kinetic parameters, one can predict the reaction rate as a function of state variables such as temperature or pressure, as long as the reaction mechanism remains the same. The underfill material used in this study is slightly modified based on previously studied underfill material [5]. In

---

* Fax: +1-480-554-5241.
E-mail address: yi.he@intel.com (Y. He).

PII: S0040-6031(00)00654-7

particular, the viscosity of the underfill encapsulant is further reduced to improve the flow characteristics.

2. Experimental

Non-isothermal and isothermal DSC experiments were performed with a Perkin-Elmer DSC7 system. Samples used for DSC experiments were sealed in aluminum hermetic pans. For non-isothermal DSC, a baseline was obtained first with empty DSC pans. For isothermal DSC, the sample was loaded into the DSC cell at room temperature, and then it was raised quickly to the isothermal temperature.

DEA experiments were performed using a TA Instruments 2970 Dielectric Analyzer with a ceramic single surface sensor. The sensor, also referred to as comb electrodes, contains an interdigitated array of excitation and response electrodes on a planar surface. Approximately 0.5 ml of sample was used each time, and the DEA gap size was 0.5 mm. The frequency used for the DEA experiments ranged from 0.1 Hz to 100 kHz. Permittivity, ε', and loss factor, ε'', were monitored as a function of temperature or time. In this study, we will focus on the position of the loss factor peak and not its absolute value, which may be related to such artifacts as sensor polarization.

3. Results and discussion

3.1. DSC curing kinetics

3.1.1. Non-isothermal DSC

DSC has been widely used to study the thermoset curing reactions [6]. The basic assumption for the application of DSC is that the measured heat flow, $\mathrm{d}H/\mathrm{d}t$, is proportional to the reaction rate, $\mathrm{d}\alpha/\mathrm{d}t$. Without knowing the exact reaction mechanism, it is reasonable to assume that the reaction rate at a given time t is only a function of the conversion fraction α, or

$$\frac{\mathrm{d}\alpha}{\mathrm{d}t} = kf(\alpha), \tag{1}$$

where k is the reaction rate constant, and is usually assumed to be of the Arrhenius form

$$k = k_0 \exp\left(-\frac{E}{RT}\right), \tag{2}$$

where k_0 is a constant, R the universal gas constant, E the activation energy, T the absolute temperature, and $f(\alpha)$ is a functional form of α depending on the reaction mechanism [6]. Based on Eq. (1), non-isothermal DSC experiments can be carried out with different heating rate, $\beta = \mathrm{d}T/\mathrm{d}t$. The activation energy E can be obtained by using the Kissinger plot [7], in which $\ln\beta$ is plotted vs. $1/T_\mathrm{p}$, where T_p is the exothermic peak temperature. The slope of the Kissinger plot is $-E/R$. The same plot can be generated based on the onset temperature for the curing reaction.

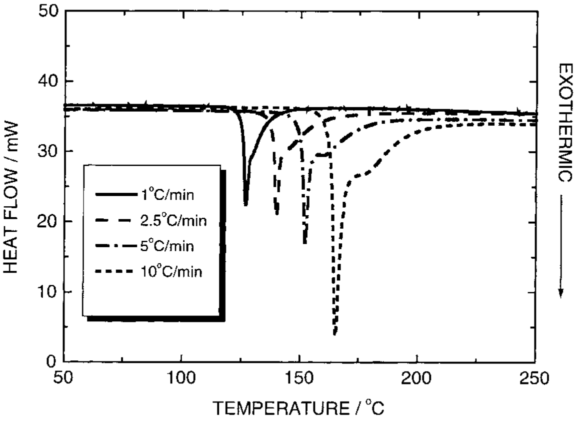

Fig. 1. Non-isothermal DSC traces of an epoxy-based underfill material.

Fig. 1 plots several non-isothermal DSC traces of the epoxy-based underfill material obtained at various heating rates. Besides the main exothermic peak, a second, smaller shoulder is also visible. Thus, it was determined that this curing reaction has at least two stages.

Fig. 2 shows the Kissinger plots based on the onset and the peak temperatures of the exothermic curing reaction, T_onset and T_p, respectively. From the slope of a linear-fit line, the activation energy, E, can be calculated. Based on the slope of the linear fit of ln b vs.$1000/T_\mathrm{p}$ E is calculated to be $87.2 \pm 2.6\,\mathrm{kJ/mol}$. When ln b vs. $1000/T_\mathrm{onset}$ $\ln\beta$ is used, E is calculated to be $88.9 \pm 2.4\,\mathrm{kJ/mol}$.

3.1.2. Isothermal DSC

From Eq. (1), the time to reach conversion α at a fixed isothermal temperature T is determined by

$$g(\alpha) = \int_0^\alpha \frac{\mathrm{d}\alpha}{f(\alpha)} = \int_0^t k\,\mathrm{d}t = kt, \tag{3}$$

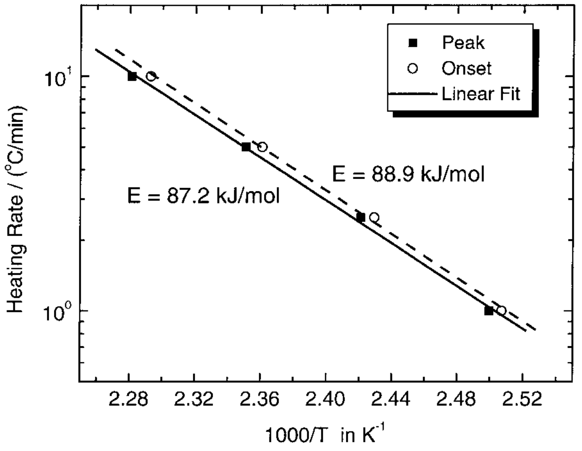

Fig. 2. Kissinger plots based on onset and peak temperatures of the main exothermic peak.

Replacing Eq. (2) into (3), we have

$$t = t_0 \exp\left(\frac{E}{RT}\right), \tag{4}$$

where t_0 is a constant for a fixed α. This means that the time to reach the same conversion fraction at different isothermal temperatures has an Arrhenius temperature dependence. This will be used to analyze isothermal DSC experiments. From Eq. (4), one can plot ln t vs. $1/T$, which should form a straight line. The slope of the line is E/R.

Isothermal DSC experiments were performed between 145 and 85°C, which covers a rather wide temperature region. Fig. 3(a) and (b) are isothermal DSC curves performed at seven different temperatures. Below 115°C, the curing reaction is not completed.

During the isothermal DSC measurement, the exothermic peak appears at a non-zero time in the isothermal segment, indicating that the curing reaction cannot be described as an nth order reaction mechanism (i.e. $f(\alpha) \neq (1-\alpha)^n$).

Based on the isothermal DSC curves, the curing onset time, t_{onset}, can be obtained. At t_{onset}, the conversion fraction α is about 5–8%. Based on the curing onset determined from isothermal DSC experiments, the activation energy E can be calculated. Fig. 4 is the plot of $\log(t_{\mathrm{onset}})$ vs. $1000/T$. The slope of the linear fit is $E/(1000R \ln 10)$. From this figure, the activation

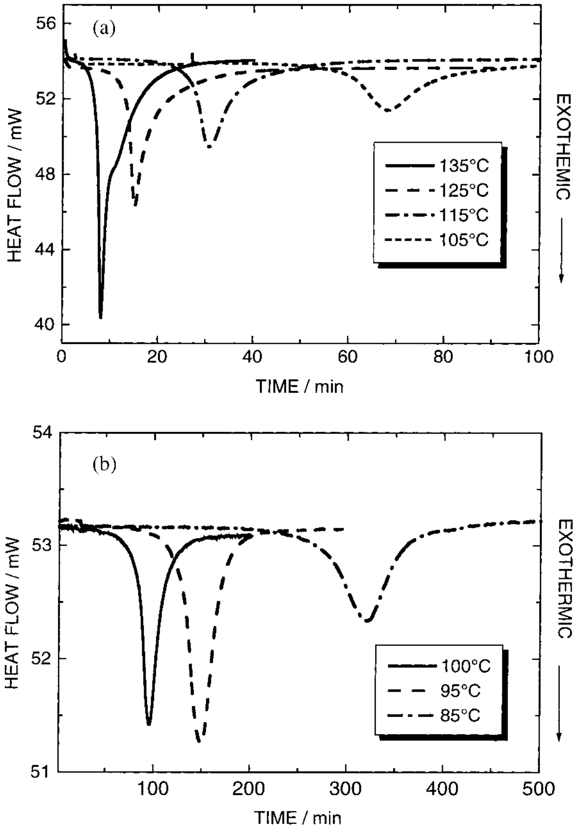

Fig. 3. Isothermal DSC results at several temperatures: (a) 135–105°C; (b) 100–85°C. The initial ramping time is excluded from the DSC curves.

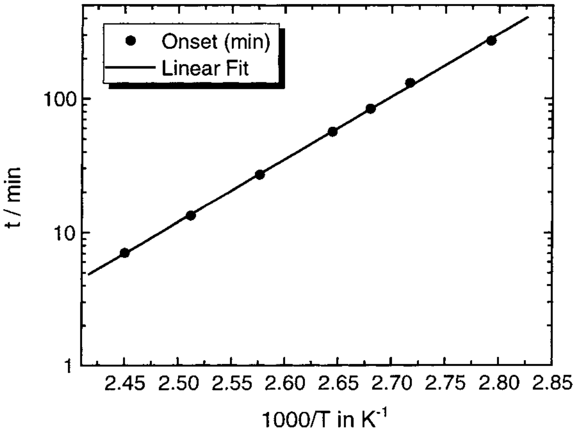

Fig. 4. Onset of isothermal DSC curing time vs. 1000/T plotted on a log-scale. Based on the slope of the linear fit, E is calculated to be 89.8 ± 0.9 kJ/mol.

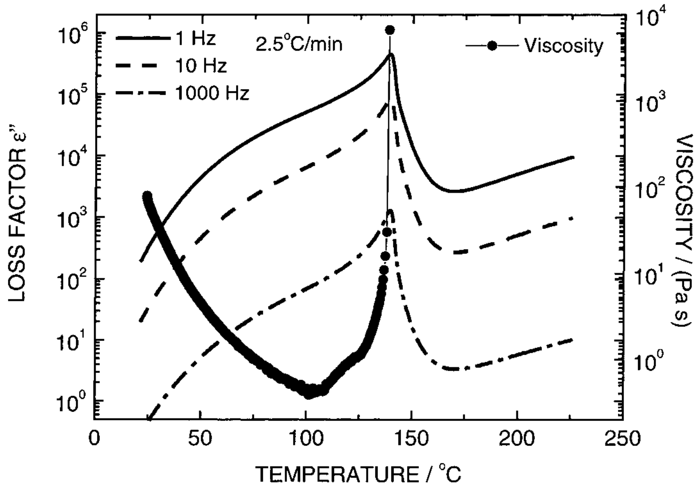

Fig. 5. ε'' curves at three different frequencies showing the curing behavior of an epoxy-based underfill material. Underfill viscosity as a function of temperature was also plotted. The ε'' peak corresponds to the gel point.

energy E is calculated to be 89.8 kJ/mol, which is in good agreement with the results obtained from the non-isothermal DSC experiments.

3.2. DEA studies of curing behavior

DEA detects changes in ionic and dipolar mobilities of a material when it is subjected to an alternating electric field. It has been used to monitor chemical reactions in organic materials for more than half of a century. In particular, it is a very useful tool to study thermoset cure [8–12], because unlike other techniques, the actual state of the material can be monitored in situ by dielectric sensing. In DEA, the capacitance and conductance of a material are measured as a function of time, temperature, and frequency. This allows the determination of electrical polarization and conduction of the material.

The dielectric data are expressed as complex dielectric constant ε^*:

$$\varepsilon^* = \varepsilon' - i\varepsilon'' \tag{5}$$

where ε' is the bulk permittivity, which measures the polarization of the material; and ε'' is the bulk loss factor, which is related to the energy loss and is related to the conductive nature of the sample; and $i = \sqrt{-1}$.

In an electric field, dipoles tend to align themselves along the direction of the field, while ions move toward the electrodes and form layers. Before the curing reaction starts, dipoles and ions can move freely. As curing proceeds, gelation takes place, thus, ions lose their translational mobility and dipoles lose their rotational mobility. Such change in ionic and dipolar mobilities during the curing process leads to the development of a peak in the loss factor curve. This peak corresponds to the onset of cure. Fig. 5 plots the DEA loss factor as a function of temperature at a heating rate of 2.5°C/min. This figure shows that the peak position in the loss factor curve is nearly frequency-independent. Also plotted in Fig. 5 is the sample viscosity curve measured by a Rheometric Scientific Rheological Dynamic Analyzer (RDA) using the same heating rate (2.5°C/min). This figure clearly demonstrated that the loss factor peak, which has a temperature of 139°C, corresponds to the gelation of the underfill epoxy, where the viscosity of the underfill epoxy increases sharply, indicating the transformation from a liquid to a gel state with increased cross-linking density. In fact, the peak positions in the DEA loss factor curves also correlate very well with the DSC curing onset, as shown in Fig. 1. Although there are different opinions concerning the ability of using DEA to determine gelation of a thermosetting system, our results suggested that at least for the underfill epoxy under this investigation, the DEA results correlate very well with rheological and calorimetric results.

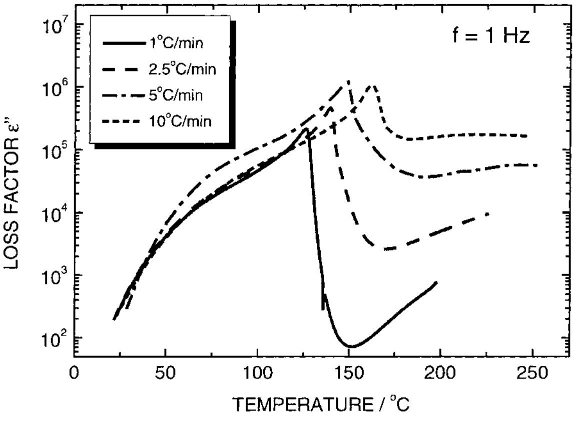

Fig. 6. ε'' vs. temperature at various heating rates. The frequency was 1 Hz.

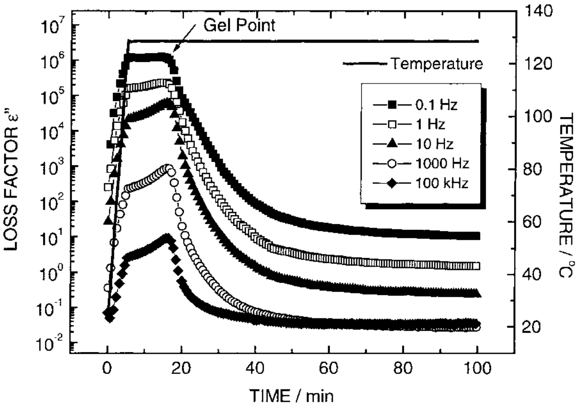

Fig. 8. Isothermal DEA curves at 128.5°C. Sample temperature was ramped from 30 to 128.5°C at a heating rate of 20°C/min.

Non-isothermal DEA experiments were also performed with heating rates of 1, 2.5, 5, and 10°C/min, as shown in Fig. 6. Similarly, Arrhenius plot can be obtained by plotting ln β vs. $1/T_p$, where T_p again is the peak temperature of the loss factor curve, and β the heating rate. Fig. 7 is the Arrhenius plot, from which the activation energy for the curing reaction is calculated to be $E = 93.0 \pm 3.1\,\mathrm{kJ/mol}$, again in good agreement with the DSC results. The small discrepancy between the DEA and DSC results may be attributed to the fact that DEA experiments required a much larger sample size (about 0.5 ml) than that was used in the DSC measurements (~20 mg).

Isothermal DEA experiments were performed between 140 and 85°C. An example is shown in Fig. 8. Similar to isothermal DSC experiments, ε'' curve develops a peak at a non-zero time in the isothermal segment, again indicating that $f(\alpha) \neq (1-\alpha)^n$. The isothermal time needed to reach the loss factor peak, t_p, is the gel time at that temperature. Again, one can plot $\ln(t_p)$ vs. $1/T$, the slope of the linear fitting is the activation energy. Fig. 9 is

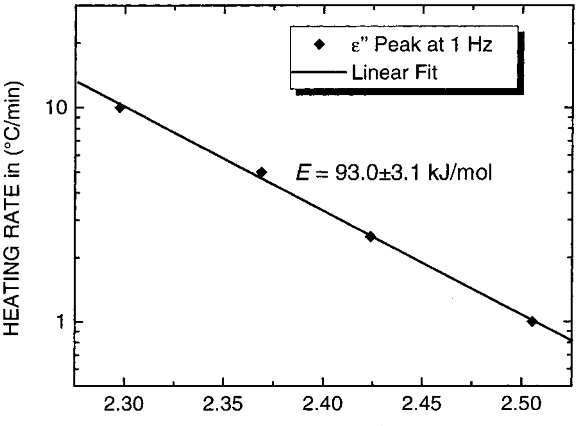

Fig. 7. Arrhenius plot based on non-isothermal DEA data. In this figure, the heating rate is plotted on a log-scale against $1000/T_p$, where T_p is the temperature corresponding to the ε'' peak. The slope of the linear fit is $E/(1000R \ln 10)$.

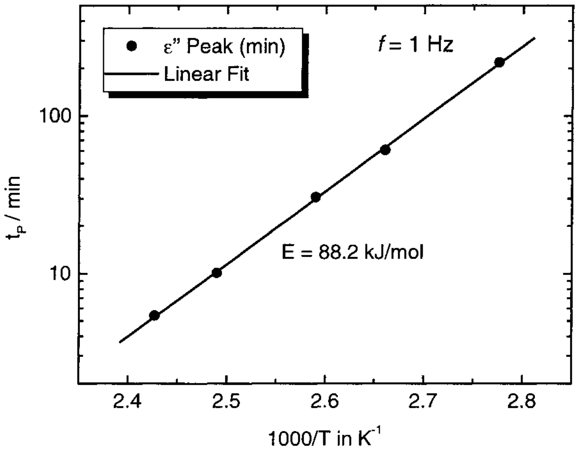

Fig. 9. Arrhenius plot based on isothermal DEA results. In this plot, the time needed to reach the loss factor peak at isothermal temperature T, which is t_p, is plotted vs. $1000/T$. The DEA frequency is 1 Hz. The ramping time to reach the isothermal temperature T from room temperature is excluded from t_p.

the Arrhenius plot based on isothermal DEA results. From this plot, the activation energy for the curing reaction can be calculated to be $E = 88.2\pm 1.0\,\mathrm{kJ/mol}$, which is in excellent agreement with the DSC results.

4. Conclusions

The curing kinetics of an epoxy-based underfill material used for flip-chip packaging has been studied using non-isothermal and isothermal DSC and DEA techniques. Experimental results revealed that the activation energy obtained from the non-isothermal DSC experiments is 87.2 kJ/mol, which is in excellent agreement with the value determined from the isothermal DSC experiments, 89.8 kJ/mol. The activation energy calculated from the non-isothermal and isothermal DEA results are 93.0 and 88.2 kJ/mol, respectively. Both results are consistent with the DSC results. Our results indicated that DSC, DEA, and rheological analysis can all be used to study the curing kinetics of the underfill epoxy used in flip-chip packaging. Furthermore, these techniques can be used to monitor the onset of curing or the gelation of the underfill epoxy, which has been identified as a critical processing parameter in electronic packaging.

Acknowledgements

The author would like to thank Brian Moreira and Stacy Nakamura for their experimental assistance during the course of this study.

References

[1] J.H. Lau, W. Nakamura, J. Prince, C.P. Wong, Electronic Packaging, Design, Materials, Process, and Reliability, McGraw-Hill, New York, 1998 (Chapter 4).

[2] A.J. Babiarz, Adv. Packaging (September/October 1998) 34.

[3] B. Potter, Adv. Packaging (February 1999) 26.

[4] J.W. Carbin, SMT (January 1999) 64.

[5] Y. He, B.E. Moreira, A. Overson, S.H. Nakamura, C. Bider, J.F. Briscoe, in: Proceedings of the 26th Conference of the North American Thermal Analysis Society, Cleveland, OH, September 13–15, 1998, pp. 345–350, Thermochin. Acta 357–358 (2000) 1.

[6] J. Barton, Adv. Polym. Sci. 72 (1985) 111.

[7] H. Kissinger, Anal. Chem. 21 (1957) 1702.

[8] D.E. Kranbuehl, in: J.P. Runt, J.J. Fitzgerald (Eds.), Dielectric Spectroscopy of Polymeric Materials: Fundamentals and Applications, American Chemical Society, Washington, DC, 1997 (Chapter 11).

[9] S.D. Senturia, N.F. Sheppard Jr., Adv. Polym. Sci. 80 (1986) 1.

[10] R.B. Prime, in: Thermal Characterization of Polymeric Materials, Vol. 2, 2nd Edition, Academic Press, San Diego, CA, 1997, pp. 1517–1537 (Chapter 6).

[11] W.W. Bidstrup, S.D. Senturia, Polym. Eng. Sci. 29 (1989) 290.

[12] D.R. Day, Polym. Eng. Sci. 29 (1989) 334.